

# Growth of Single-Crystal $\text{Ca}_{10}(\text{Pt}_4\text{As}_8)(\text{Fe}_{1.8}\text{Pt}_{0.2}\text{As}_2)_5$ Nanowhiskers with Superconductivity up to 33 K

Jun Li,<sup>†,‡</sup> Jie Yuan,<sup>†</sup> Dai-Ming Tang,<sup>#</sup> Shou-Bao Zhang,<sup>#,⊥,||</sup> Meng-Yue Li,<sup>†,§</sup> Yan-Feng Guo,<sup>#,⊥</sup> Yoshihiro Tsujimoto,<sup>#</sup> Takeshi Hatano,<sup>†</sup> Shunichi Arisawa,<sup>†</sup> Dmitri Golberg,<sup>#</sup> Hua-Bing Wang,<sup>\*,†,§</sup> Kazunari Yamaura,<sup>\*,†,‡,#,⊥</sup> and Eiji Takayama-Muromachi<sup>‡,‡,⊥</sup>

<sup>†</sup>Superconducting Properties Unit, National Institute for Materials Science, 1-1 Namiki, Tsukuba, Ibaraki 305-0044, Japan

<sup>‡</sup>Department of Chemistry, Graduate School of Science, Hokkaido University, Sapporo, Hokkaido 060-0810, Japan

<sup>#</sup>International Center for Materials Nanoarchitectonics (MANA), National Institute for Materials Science, 1-1 Namiki, Tsukuba, Ibaraki 305-0044, Japan

<sup>⊥</sup>JST, Transformative Research-Project on Iron Pnictides (TRIP), 1-1 Namiki, Tsukuba, Ibaraki 305-0044, Japan

<sup>§</sup>Research Institute of Superconductor Electronics, Nanjing University, Nanjing 210093, China

## Supporting Information

**ABSTRACT:** Single-crystal  $\text{Ca}_{10}(\text{Pt}_4\text{As}_8)(\text{Fe}_{1.8}\text{Pt}_{0.2}\text{As}_2)_5$  superconducting (SC) nanowhiskers with widths down to hundreds of nanometers were successfully grown in a Ta capsule in an evacuated quartz tube by a flux method. Magnetic and electrical properties measurements demonstrate that the whiskers have excellent crystallinity with critical temperature of up to 33 K, upper critical field of 52.8 T, and critical current density of  $J_c$  of  $6.0 \times 10^5$  A/cm<sup>2</sup> (at 26 K). Since cuprate high- $T_c$  SC whiskers are fragile ceramics, the present intermetallic SC whiskers with high  $T_c$  have better opportunities for device applications. Moreover, although the growth mechanism is not understood well, the technique can be potentially useful for growth of other whiskers containing toxic elements.

Shrinking to the nanoscale often leads to new fundamental phenomena: to name a few, the global phase coherence in superconducting (SC) nanocylinders,<sup>1</sup> the quantization of the Bose condensate,<sup>2</sup> the dynamics of the SC condensate,<sup>3</sup> the paramagnetic Meissner effect in micrometer-size superconductors,<sup>4</sup> and the critical dimensionality effect on the superconductivity.<sup>5</sup> Thus, although most studies on superconductivity have been focused on bulk materials and thin films,<sup>6,7</sup> it would be highly valuable to investigate the phenomenon in one-dimensional (1-D) nanostructures such as nanowires, nanotapes, and nanowhiskers. These structures could find practical applications in electrical devices as SC magnets or as materials for energy transportation and storage since 1-D superconductors show very high critical currents.<sup>8,9</sup> Moreover, once the anisotropic property is strong enough, it may be possible to observe intrinsic Josephson effects as in cuprate superconductors.<sup>9</sup>

Regarding the material itself, Fe-based superconductors are of particular interest since their discovery led to unexpectedly rapid development in superconductivity research. This was because of the strong desire to explain the mechanism behind the high-transition-temperature ( $T_c$ ) superconductivity as well as to establish reliable production methods toward useful

applications.<sup>10–13</sup> However, thus far, only one group has explored 1-D Fe-based superconductors, specifically, F-doped  $\text{SmFeAsO}$  nanocables fabricated using  $\text{ZnO}$  nanotubes as a template.<sup>14</sup> However, the SC properties of this material remain uncertain because of the absence of transport property characteristics and detailed structural analyses. Furthermore, it is generally hard to synthesize 1-D structures of Fe-based superconductors because of difficulties in controlling the composition, stoichiometry, and/or crystal structure. Even for the cuprate family, 1-D superconductors have been fabricated only via very specialized techniques such as electron beam lithography,<sup>15</sup> biomimetic process,<sup>16</sup> and the sol–gel method combined with a template.<sup>17</sup> Thus, instead of the difficult-to-fabricate nanostructures, SC whiskers with widths on the order of several tens of micrometers have been comprehensively studied, especially for the Bi–Sr–Ca–Cu–O (BSCCO) system.<sup>8,9</sup>

Recently,  $\text{Ca}_{10}(\text{Pt}_4\text{As}_8)(\text{Fe}_{2-x}\text{Pt}_x\text{As}_2)_5$  superconductors were found to crystallize into a layered structure with an infinite sequence of  $-\text{Ca}-(\text{Pt}_4\text{As}_8)-\text{Ca}-\text{Fe}_{2-x}\text{Pt}_x\text{As}_2-$  units, where the intermediate  $\text{Pt}_4\text{As}_8$  layer produced unusual structural and metallic characteristics.<sup>18–21</sup> It was pointed out that such metallic intermediate layers may be a promising tool to obtain much higher  $T_c$ 's.<sup>19</sup> Motivated by the prospect, we focused our efforts on growing crystals of the superconductor. As a result, successful growth of whiskers was achieved in a Ta capsule in an evacuated quartz tube by a flux method. Neither gas nor evaporation was used to transport elements as in well-established methods, thus reducing the risk of human exposure to toxic As. Here, we report the synthesis and characterization of the  $\text{Ca}_{10}(\text{Pt}_4\text{As}_8)(\text{Fe}_{1.8}\text{Pt}_{0.2}\text{As}_2)_5$  nanowhiskers. To our knowledge, these are the first nanoscale SC whiskers synthesized from a material in the Fe-based superconductor family.

Single-crystal whiskers of  $\text{Ca}_{10}(\text{Pt}_4\text{As}_8)(\text{Fe}_{2-x}\text{Pt}_x\text{As}_2)_5$  ( $x = 0, 0.1, 0.2, 0.3,$  and  $0.36$ ) were prepared by a flux method. The

Received: December 26, 2011

Published: February 17, 2012

starting materials—CaAs (lab made by the same preparation process as reported in ref 22), FeAs (lab made<sup>22</sup>), Fe (3N), and Pt (3N)—were mixed and placed in an h-BN cell,<sup>22</sup> which was sealed in a Ta capsule (Ta thickness is 0.2 mm) by using punches and a die (the applied pressure to the capsule was 380 MPa; see details in Figure 1S in Supporting Information [SI]). Here, 10 wt% of additional CaAs was used as a flux. After removing the pressure, the sealed capsule, in turn, was placed in an evacuated quartz tube. The loaded capsule was heat-treated at 1000 °C for 72 h and then slowly cooled to 700 °C over 48 h. Whiskers were found at the surface of the as-prepared bulk samples inside the capsule with substitution of Pt for  $x > 0.1$ , among which  $\text{Ca}_{10}(\text{Pt}_4\text{As}_8)(\text{Fe}_{1.8}\text{Pt}_{0.2}\text{As}_2)_5$  had the best crystallinity and superconductivity (Figure 1a,b). Note that

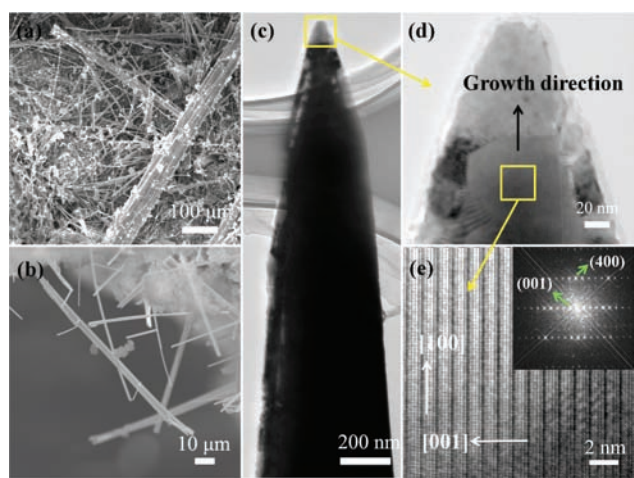


**Figure 1.** (a) and (b) SEM images of whiskers. (c) TEM image of a whisker with a width of  $\sim 500$  nm, and (d) enlarged view of the tip. (e) High-resolution image of the crystalline core that shows growth occurred along the  $[100]$  direction, with the corresponding SAED pattern in the inset.

the whiskers can only grow at the sealing pressures of 260–480 MPa, suggesting that an internal stress may also play a substantial role in the whisker growth.

In the present experiments, the addition of appropriate amounts of CaAs and stress seem to be the most integral conditions for growth of the whiskers. However, note that the complete formation mechanism is not understood at present and additional work is needed to elucidate the actual mechanism. Nevertheless, a possible explanation is presented here for the sake of discussion: We consider that a liquid-phase reaction occurs in the isolated Ta/BN capsule during the isothermal process at 1000 °C. On cooling, bulk crystals form in the CaAs flux, resulting in large shrinkage of the capsule. Consequently, during the cooling process, the actual vapor pressure may increase allowing whiskers to grow from the bulk crystals, together with various 1-D structures, in a vapor–liquid–solid process.<sup>23–25</sup>

The typical  $\text{Ca}_{10}(\text{Pt}_4\text{As}_8)(\text{Fe}_{1.8}\text{Pt}_{0.2}\text{As}_2)_5$  whiskers obtained had a length ( $L$ ) of 0.1–2.0 mm, width ( $d$ ) of 0.4–5.0  $\mu\text{m}$ , and thickness ( $h$ ) of 0.2–1.0  $\mu\text{m}$ . Structural characterization of individual whiskers was accomplished by transmission electron microscopy (Figure 1c), which revealed a sharp tip with a width of around 30 nm. The magnified image of the tip in Figure 1d reveals that the whisker has a single-crystal core and a polycrystalline or amorphous shell with thickness of about 20

nm. However, magnified images of another edge show the polycrystalline or amorphous shell is less than 5 nm in thickness [Figure 2Sc, SI], being much thinner than that of the tip part. Such a polycrystalline or amorphous shell therefore hardly impacts on the properties of the whiskers. The high-resolution image of the core, as shown in Figure 1e, reveals a clear, multilayered structure parallel to the whisker axis. Furthermore, the selected-area electron-diffraction (SAED) pattern was obtained from the corresponding selected area as shown in the inset to Figure 1e, which was consistent with the  $\text{SrZnSb}_2$ -type structure reported for the bulk material.<sup>19</sup> The SAED patterns at seven places show the almost identical diffraction patterns corresponding to the  $[001]$  zone axis (Figure 3S, SI), indicating that the whole whisker is single crystalline and the growth direction is along  $ab$  axis. The result of spatially resolved energy dispersive X-ray spectroscopy is given in Figure 2Sb (SI), where the semiquantitative analysis demonstrates that Ca/Fe/Pt/As atomic ratio of 2:1.2:0.3:0.6 is slightly different from the starting composition. Consequently, we can conclude that the growth direction of the whisker is along the  $[100]$  direction ( $ab$ -axis), and the direction perpendicular to the whisker axis is  $[001]$ , namely, the  $c$ -axis.

Powder X-ray diffraction (XRD) pattern (Figure 2) obtained from an amount of ground whiskers were well characterized by

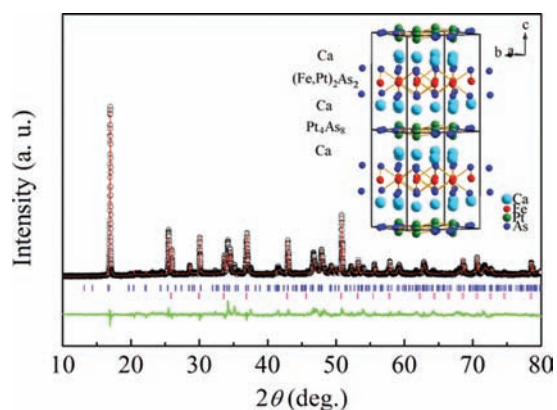


**Figure 2.** Powder XRD pattern and its Rietveld refinement for the whiskers. The data (black open symbols), the profile calculated after refinements (red line), the refined data for  $\text{Ca}_{10}(\text{Pt}_4\text{As}_8)(\text{Fe}_{1.8}\text{Pt}_{0.2}\text{As}_2)_5$  (blue dashes) and  $\text{PtAs}_2$  (pink dashes), and their differences (green line). Inset is the lattice structure model (ref 19) used in the refinement for the XRD pattern.

assuming the  $\text{SrZnSb}_2$ -type structure model ( $P4/n$ ), which was proposed for a bulk crystal.<sup>18–20</sup> However, Rietveld refinement of the pattern resulted in a fair fitting quality (Rp: 11.012, Rwp: 13.325) probably because of the limited sample mass in a laboratory XRD instrument. Perhaps, a synchrotron XRD study may help to test the structure model on the whisker. Nevertheless, lattice parameters for the whiskers were determined to be  $a = 8.7176(3)$  Å and  $c = 10.5327(4)$  Å, close to the values reported previously.<sup>19</sup> Note nontrivial amount of impurity, presumably  $\text{PtAs}_2$ , was detected in the pattern ( $\sim 19$  mass %). This was because the impurities could not be easily separated when collecting the crystals.

Next, DC magnetic susceptibility ( $\chi$ ) measurements were carried out using a Magnetic Properties Measurement System from Quantum Design. Since the size of an individual whisker is too small for accurate measurements, we gathered a number of whiskers into a sample holder. As shown in Figure 3a, the

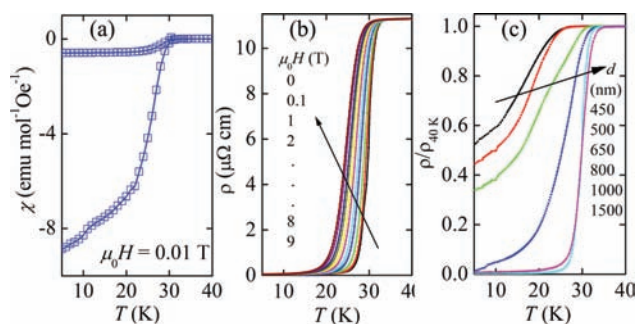


**Figure 3.** (a)  $\chi$  vs  $T$  for gathered whiskers. (b)  $\rho$  vs  $T$  for an individual whisker in various magnetic fields ( $d = 1000$  nm,  $h = 500$  nm). (c) Normalized resistance vs  $T$  for whiskers of various widths ( $I = 0.5$  mA).

temperature ( $T$ ) dependence of  $\chi$  in a magnetic field of 0.01 T shows a clear SC transition at 33 K. The estimated shielding fraction is fairly small, being 23% (at 2 K) of perfect diamagnetism. This is probably because the measurement is affected by the extremely anisotropic shape of the crystals.

As shown in Figure 3b, we measured the temperature dependence of ac-electrical resistivity ( $\rho$ ) for individual whiskers using a Physical Property Measurement System from Quantum Design (the measurement details are shown in Figure 4S). Here, the magnetic field was applied perpendicular to the wide-face ( $L \times d$ ) of the whisker. The obtained  $T_c$  of 33 K matches the result of the magnetic measurements. Then, using the Werthamer–Helfand–Hohenberg (WHH) model,<sup>26</sup> we roughly estimated the upper critical field ( $H_{c2}$ ) as 52.8 T (Figure 5S). An angular-dependent magnetoresistance measurement by rotating the whisker along the  $a$ - or  $b$ -axis (Figure 6S) shows the minimum and the maximum resistivity by turns at every 90° step, suggesting that the wide-face is indeed the  $ab$ -plane. Consequently,  $H_{c2}$  can be denoted as  $H_{c2}^{\perp ab}$ , which is larger than that for the bulk material (13 T).<sup>19</sup> We also estimated the critical current density ( $J_c$ ) from the current–voltage ( $I$ – $V$ ) characteristics;  $J_c$  was relatively high, for instance,  $6.0 \times 10^5$  A/cm<sup>2</sup> at 26 K. Because the enhancement mechanism of  $H_{c2}$  and  $J_c$  is not yet clear, studies of intrinsic flux pinning and vortex avalanches<sup>27</sup> and geometric barrier regarding the unusual shape of the crystal are in progress.

We measured the  $\rho$  of whiskers with various widths, as shown in Figure 3c. Despite the clear SC transition, zero resistance is not obtained in the whiskers with  $d < 1$   $\mu$ m. Since  $d$  is at the nanoscale, the current density may approach the critical value and hence weaken the superconductivity. To probe the issue further, we attempted measurements at much lower gauge currents—down to 1  $\mu$ A. However, the observed transport properties were found to be highly complicated, probably because of the significant domain scattering or system noise—the critical current of nanoscale whiskers is highly sensitive to the current bias. Additional studies are in progress.

In summary, single-crystal SC whiskers of  $\text{Ca}_{10}(\text{Pt}_4\text{As}_8)(\text{Fe}_{1.8}\text{Pt}_{0.2}\text{As}_2)_5$  were grown in a Ta capsule in an evacuated quartz tube by a flux method. This technique can be potentially useful for growth of other whiskers containing toxic elements, although the growth mechanism is not understood well. The  $\text{Ca}_{10}(\text{Pt}_4\text{As}_8)(\text{Fe}_{1.8}\text{Pt}_{0.2}\text{As}_2)_5$  whiskers were confirmed to have excellent crystallinity with  $T_c$  of 33 K,  $H_{c2}^{\perp ab}$  of 52.8 T, and  $J_c$  of  $6.0 \times 10^5$  A/cm<sup>2</sup> (at 26 K). The  $T_c$  value is comparable with that of the bulk material; however, the  $H_{c2}^{\perp ab}$  is 3 times higher.

Since cuprate high- $T_c$  SC whiskers are fragile ceramics, the present intermetallic SC whiskers with high  $T_c$  have better opportunities for device applications.

## ASSOCIATED CONTENT

### Supporting Information

Sample fabrication and measurement details. This material is available free of charge via the Internet at <http://pubs.acs.org>.

## AUTHOR INFORMATION

### Corresponding Author

wang.huabing@nims.go.jp; yamaura.kazunari@nims.go.jp

### Present Address

<sup>||</sup>Institute for Chemical Research, Kyoto University, Gokasho, Uji, Kyoto 611–0011, Japan.

### Notes

The authors declare no competing financial interest.

## ACKNOWLEDGMENTS

We thank Dr. H. Kontani for the valuable discussions. We also thank Dr. K. Kosuda for the EMPA measurements and Dr. A. S. Sato for the XRD measurements. This research was supported in part by the World Premier International Research Center from MEXT, Grants-in-Aid for Scientific Research (22246083) from JSPS, and the Funding Program for World-Leading Innovative R&D on Science and Technology (FIRST Program) from JSPS.

## REFERENCES

- Lee, S.; Jiang, J.; Zhang, Y.; Bark, C. W.; Weiss, J. D.; Tarantini, C.; Nelson, C. T.; Jang, H. W.; Folkman, C. M.; Baek, S. H.; Polyanskii, A.; Abrahimov, D.; Yamamoto, A.; Park, J. W.; Pan, X. Q.; Hellstrom, E. E.; Larbalestier, D. C.; Eom, C. B. *Nat. Mater.* **2010**, *9*, 397.
- Geim, A. K.; Grigorieva, I. V.; Dubonos, S. V.; Lok, J. G. S.; Maan, J. C.; Filippov, A. E.; Peeters, F. M. *Nature* **1997**, *390*, 259.
- Vodolazov, D. Y.; Peeters, F. M.; Piraux, L.; Mátéfi-Tempfli, S.; Michotte, S. *Phys. Rev. Lett.* **2003**, *91*, 157001.
- Geim, A. K.; Dubonos, S. V.; Lok, J. G. S.; Henini, M.; Maan, J. C. *Nature* **1998**, *396*, 144.
- Sobnack, M. B.; Kusmartsev, F. V. *Phys. Rev. Lett.* **2001**, *86*, 716.
- Baily, S. A.; Kohama, Y.; Hiramatsu, H.; Maiorov, B.; Balakirev, F.; Hirano, M.; Hosono, H. *Phys. Rev. Lett.* **2009**, *102*, 117004.
- Liu, Y.; Zadorozhny, Yu.; Rosario, M. M.; Rock, B. Y.; Carrigan, P. T.; Wang, H. *Science* **2001**, *294*, 2332.
- Nagao, M.; Sato, M.; Maeda, H.; Kim, S. J.; Yamashita, T. *Appl. Phys. Lett.* **2001**, *79*, 16.
- Latyshev, Y. I.; Orlov, A. P.; Nikitina, A. M.; Monceau, P.; Klemm, R. A. *Phys. Rev. B* **2004**, *70*, 094517.
- Kamihara, Y.; Watanabe, T.; Hirano, M.; Hosono, H. *J. Am. Chem. Soc.* **2008**, *130*, 3296.
- Rotter, M.; Tegel, M.; Johrendt, D. *Phys. Rev. Lett.* **2008**, *101*, 107006.
- Ren, Z. A.; Lu, W.; Yang, J.; Yi, W.; Shen, X. L.; Zheng, C.; Che, G. C.; Dong, X. L.; Sun, L. L.; Zhou, F.; Zhao, Z. X. *Chin. Phys. Lett.* **2008**, *25*, 2215.
- Mazin, I. I. *Nature* **2010**, *464*, 183.
- Zhou, S.-M.; Li, S.; Wang, P.; Zhao, D.-Q.; Gong, H.-C.; Zhang, B.; Wang, M.; Zhang, X.-T. *Supercond. Sci. Technol.* **2008**, *21*, 125007.
- Bonetti, J. A.; Caplan, D. S.; Harlingen, D. J.; Van, Weissman, M. B. *Phys. Rev. Lett.* **2004**, *93*, 087002.
- Hall, S. R. *Adv. Mater.* **2006**, *18*, 487.
- Lu, X.; Zhang, T.; Qu, J.; Jin, C.; Li, X. G. *Adv. Funct. Mater.* **2006**, *16*, 1754.

- (18) Kakiya, S.; Kudo, K.; Nishikubo, Y.; Oku, K.; Nishibori, E.; Sawa, H.; Amamoto, T.; Nozaka, T.; Nohara, M. *J. Phys. Soc. Jpn.* **2011**, *80*, 093704.
- (19) Ni, N.; Allred, J. M.; Chan, B. C.; Cava, R. J. *Proc. Natl. Acad. Sci. U.S.A.* **2011**, *108*, E1019.
- (20) Löhnert, C.; Stürzer, T.; Tegel, M.; Frankovsky, R.; Friederichs, G.; Johrendt, D. *Angew. Chem., Int. Ed.* **2011**, *50*, 9195.
- (21) Kawamata, T.; Iida, T.; Suzuki, K.; Satomi, E.; Kobayashi, Y.; Itoh, M. *J. Phys. Soc. Jpn.* **2011**, *80*, 073710.
- (22) Li, J.; Guo, Y. F.; Zhang, S. B.; Yu, S.; Tsujimoto, Y.; Kontani, H.; Yamaura, K.; Takayama-Muromachi, E. *Phys. Rev. B* **2011**, *84*, 020513(R).
- (23) Joshi, U. A.; Lee, J. S. *Small* **2005**, *1*, 1172.
- (24) Mao, Y.; Banerjee, S.; Wong, S. S. *J. Am. Chem. Soc.* **2003**, *125*, 15718.
- (25) Zhu, X.; Liu, Z.; Ming, N. *J. Mater. Chem.* **2010**, *20*, 4015.
- (26) Werthamer, N. R.; Helfand, E.; Hohenberg, P. C. *Phys. Rev.* **1966**, *147*, 295.
- (27) Wang, X.-L.; Ghorbani, S. R.; Lee, S.-I.; Dou, S. X.; Lin, C. T.; Johansen, T. H.; Müller, K.-H.; Cheng, Z. X.; Peleckis, G.; Shabazi, M.; Qyiller, A. J.; Yurchenko, V. V.; Sun, G. L.; Sun, D. L. *Phys. Rev. B* **2010**, *82*, 024525.